BOLLETTINO DI GEOFISICA TEORICA ED APPLICATA VOL. XXXIV, N. 136 - DECEMBER 1992

G. CASULA and J. M. CARCIONE

GENERALIZED MECHANICAL MODEL ANALOGIES OF LINEAR VISCOELASTIC BEHAVIOUR

Abstract: The description of wave propagation by a viscoelastic rheology allows for the introduction of two important phenomena: wave dissipation, i.e., the conversion of motion into heat, and velocity dispersion, the phenomenon in which two different Fourier components travel with different velocities. In this work, we consider a mechanical representation of viscoelastic media, which in virtue of its simplicity constitutes a useful tool to model the variety of dissipation mechanisms present in real media. Examples of simulated wavefields in these types of media can be found, for instance, in the works of Carcione et al. (1988 a,b), where the equations are based on the standard linear solid model. Here we analyze in detail the physical properties and capabilities of different mechanical models, and give some hints to obtain realistic models of attenuation and velocity dispersion; for example, the constant Q phenomenon and the set of relaxation peaks over a given frequency band.

INTRODUCTION

Anelasticity usually depends on a large number of physical mechanisms, which can be modelled by different microstructural theories. A general way to include all these mechanisms is to use a phenomenological model to describe the rheology of the medium. A model which is consistent with the physical properties of real media is represented mechanically by the standard linear solid. A general linear viscoelastic solid can be obtained by considering several standard linear mechanisms in parallel or in series. The resulting anelastic material is then represented by the most linear relation between stress and strain. This paper treats in detail the different mechanical representations of viscoelastic materials, analysing their capacity to represent the behaviour of real anelastic media.

Viscoelastic behaviour is a time-dependent, mechanical non-instantaneous response of a material body to variations of applied stress deformation. Because the response is not instantaneous, there is a time dependent function that characterizes the behaviour of the material. The function contains the stress or strain history of the viscoelastic body. The strength of the dependence is greater for events in the most recent past and diminishes as they become more remote in time: it is said that the material has memory. In a linear viscoelastic material, the stress is linearly related to the strain history until a given time. The strain arising from any increment of the stress will add to the strain resulting from stresses previously created in the body. This is expressed in mathematical form by Boltzmann's superposition principle, which in 1-D space is given by (e.g. Christensen, 1982)

$$\sigma = \psi * \dot{\epsilon} \qquad (1)$$

Manuscript received September 6, 1992; accepted December 10, 1992.

Osservatorio Geofisico Sperimentale, P.O. Box 2011, Opicina, 34016 Trieste, Italy.

or

$$\epsilon = \chi * \dot{\sigma}, \tag{2}$$

where σ is the stress, ϵ is the strain, and ψ and χ are the relaxation and creep functions, respectively. The symbol '*' denotes time convolution and the dot above a function represents time differentiation. Applying properties of the convolution (e.g. Bracewell, 1965) and transforming eqns. (1) and (2) to the frequency-domain yields

$$\tilde{\sigma} = Y\tilde{\epsilon} \tag{3}$$

and

$$\tilde{\epsilon} = J\tilde{\sigma}, \tag{4}$$

where

$$Y(\omega) = \int_{-\infty}^{+\infty} \dot{\psi}(t)\, e^{-i\omega t} dt \tag{5}$$

is the complex relaxation modulus, and

$$J(\omega) = \int_{-\infty}^{+\infty} \dot{\chi}(t)\, e^{-i\omega t} dt \tag{6}$$

is the complex creep compliance, where ω is the angular frequency and t is the time variable. Note that $J(\omega)^{-1} = Y(\omega)$. The anelastic effects are quantified by the quality factor and the phase velocity dispersion. The quality factor is the peak potential energy density divided by the loss energy density, and is given by (e.g., Ben-Menahem and Singh, 1981; Carcione et al., 1988b)

$$Q(\omega) = \frac{\mathrm{Re}\,[Y(\omega)]}{\mathrm{Im}\,[Y(\omega)]}, \tag{7}$$

where 'Re' and 'Im' are the real and imaginary parts, respectively. The phase velocity for a homogeneous viscoelastic plane wave is the angular frequency divided by the real wavenumber (see Appendix A):

$$V_p(\omega) = \left(\mathrm{Re}\left[V(\omega)^{-1}\right]\right)^{-1}, \quad V(\omega) = \sqrt{\frac{Y(\omega)}{\varrho}}, \tag{8}$$

where $V(\omega)$ is the complex velocity and ϱ is the medium density.

This paper is organized as follows: the first three sections describe the basic mechanical models; Maxwell, Kelvin-Voigt and standard linear solid. We compute quality factor, phase and group velocities and creep and relaxation functions which are the relevant experimental indicators for wave and static problems, respectively.

Finally, in the last section, we analyse the general standard linear solid for obtaining a set of relaxation mechanisms and constant Q behaviour.

MECHANICAL MODELS OF VISCOELASTIC BEHAVIOUR

The objective is to obtain a consitutive relation which can explain, for instance, the typical relaxation spectrum and creep function shown in Figs. 1 and 2, respectively. Many peaks are

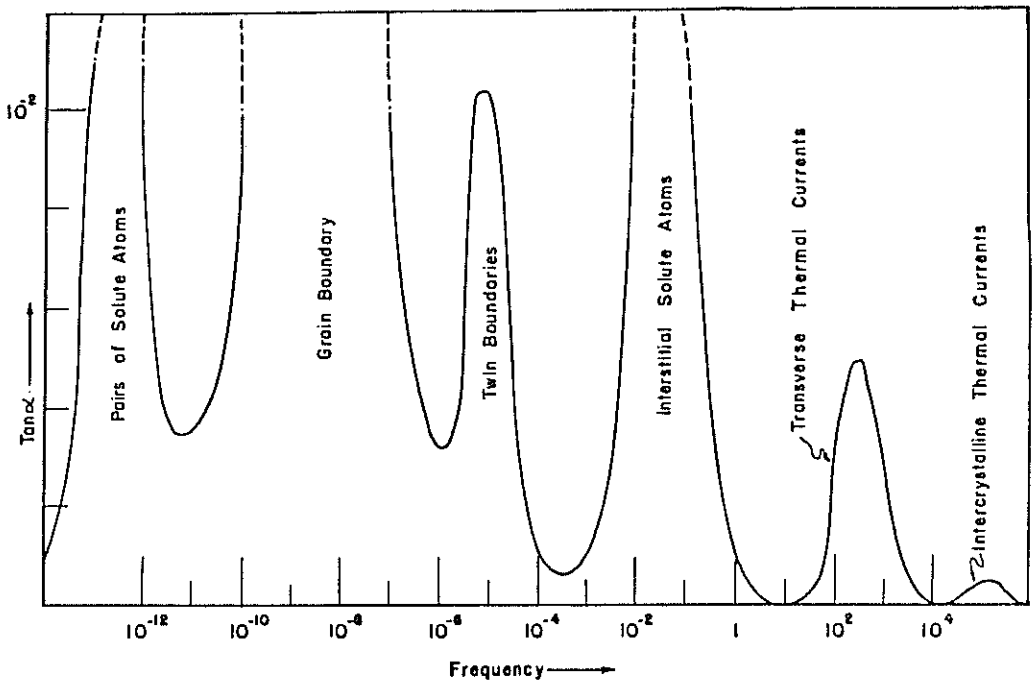

Fig. 1 — A typical relaxation spectrum (Zener, 1948).

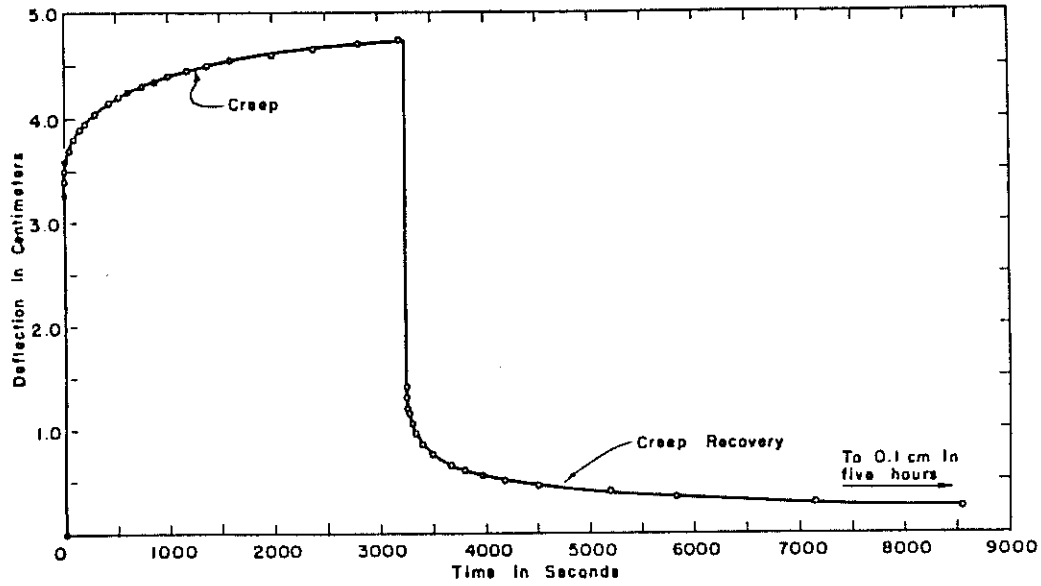

Fig. 2 — Creep function under constant stress and creep recovery in polycrystalline alluminium (Zener, 1948).

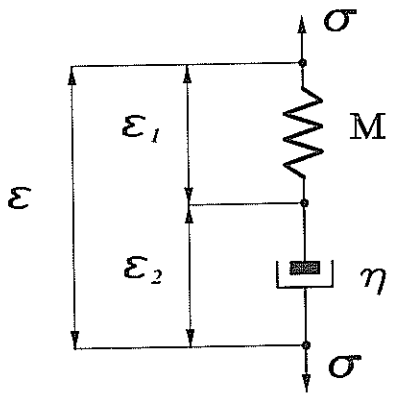

Fig. 3 — Mechanical model for a Maxwell substance. The force on both elements is the same but the elongation (strain) is different.

seen in the internal friction versus frequency curve, each of which can be attributed to a different relaxation process. Complex modulus, quality factor, phase and group velocities, relaxation and creep functions are analysed for the Maxwell, Kelvin-Voigt, standard linear solid and general standard linear solid models.

The Maxwell model was introduced by Maxwell (1868) when discussing the nature of viscosity in gases. Meyer (1878) and Voigt (1892) obtained the so called Voight constitutive relation by generalizing the equations of the classical elasticity theory. The mechanical model representation of the Voigt solid (the Kelvin-Voigt model) was obtained by Thomson (1875).

Maxwell model

To construct a mechanical model analogue, two types of basic element are required: weightless springs (no inertial effects are present), which represent the elastic solid, and dashpots consisting of loosely fitting pistons in cylinders filled with a viscous fluid. The simplest series combi-

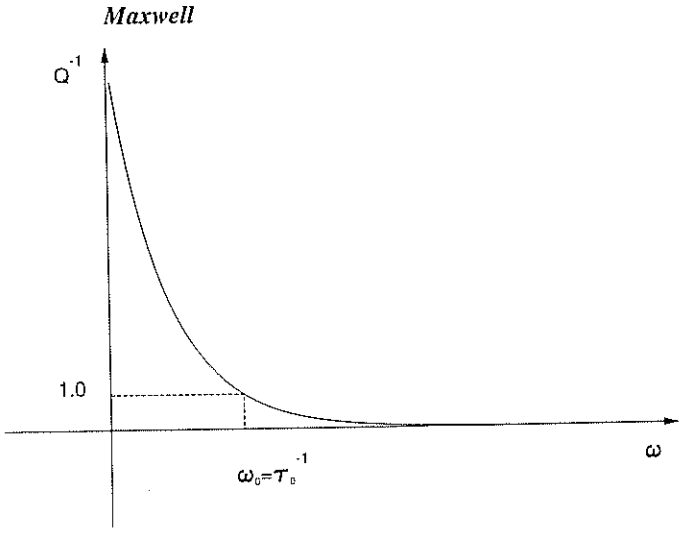

Fig. 4 — Dissipation factor of the Maxwell model. The system acts as a low-pass filter since high frequency modes dissipate completely.

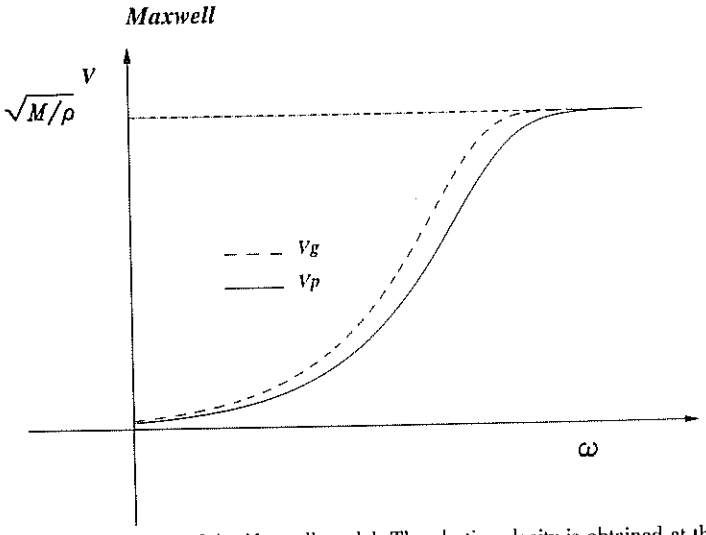

Fig. 5— Phase and group velocities of the Maxwell model. The elastic velocity is obtained at the high frequency limit. At the low frequency limit there is no propagation.

nation of these two elements which represents viscoelastic behavior is the Maxwell model depicted in Fig. 3. A given stress σ applied to the model produces a deformation ϵ_1 on the spring and a deformation ϵ_2 on the dashpot. The stress-strain relation in the spring is $\sigma=M\epsilon_1$, where M is the elastic modulus, and $\sigma=\eta\dot{\epsilon}_2$ in the dashpot, with η the viscosity. Assuming that the total elongation of the system is $\epsilon=\epsilon_1+\epsilon_2$, the constitutive relation of the Maxwell element is

$$\frac{\dot{\sigma}}{M}+\frac{\sigma}{\eta}=\dot{\epsilon}. \tag{9}$$

Performing the time Fourier transform of eqn. (9), we obtain the stress-strain relation in the frequency domain:

$$\tilde{\sigma}=\frac{\omega\eta}{(\omega\tau_0-i)}\tilde{\epsilon}, \tag{10}$$

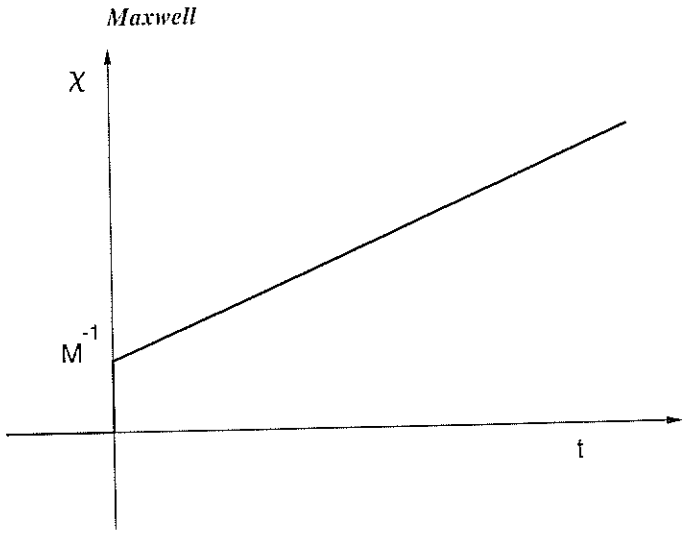

Fig. 6 — The creep function of the Maxwell model resembles the creep function of a viscous fluid.

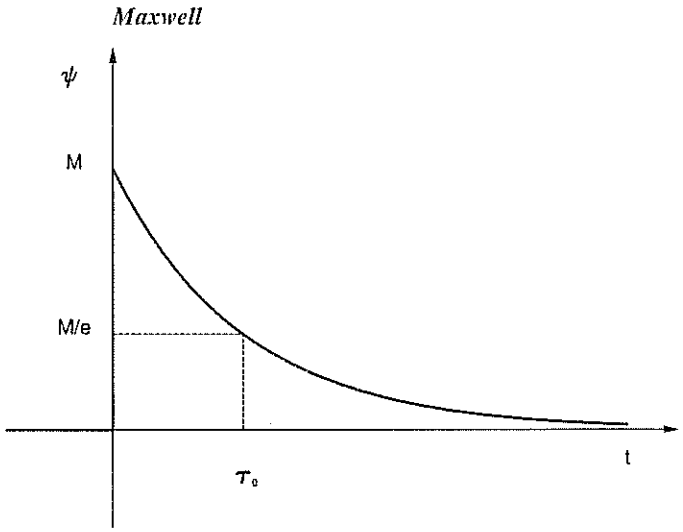

Fig. 7 — Relaxation function of the Maxwell model. The system does not present an asymptotical residual stress as in the case of real solids.

where $\tau_0=\eta/M$ is a relaxation time. Using the correspondence principle (Flugge, 1960), the complex modulus is identified as

$$Y(\omega)=\frac{\omega\eta}{\omega\tau_0-i}\ . \tag{11}$$

The spatial quality factor (7) is then

$$Q(\omega)=\omega\tau_0\ . \tag{12}$$

Fig. 4 shows the dissipation factor Q^{-1} as a function of frequency. The phase velocity, represented in Fig. 5, is obtained by inserting the complex modulus (11) into eqn. (8). When $\omega\to 0$, $V_p\to 0$, and $\omega\to\infty$, then $V_p\to (M/\varrho)^{1/2}$, the elastic velocity, assuming that only the spring is considered. This implies that a wave in a Maxwell material travels slower than a wave in an elastic material (provided that the elastic case is the low frequency limit). The group velocity, or velocity of the wave packet, is given by (Appendix A)

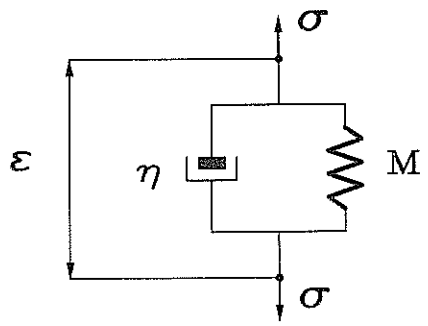

Kelvin-Voigt Model

Fig. 8 — Mechanical model for a Kelvin-Voigt substance. The strain is the same but the forces are different.

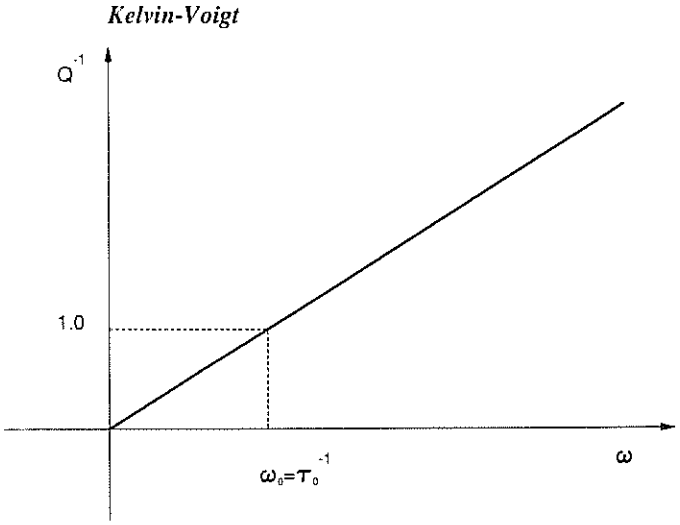

Fig. 9 — Dissipation factor of the Kelvin-Voigt model. The system acts as a high pass filter since low frequency modes dissipate completely.

$$V_g(\omega) = \left(\mathrm{Re}\left[V(\omega)^{-1} \left(1 - \frac{\omega}{2} \frac{Y'(\omega)}{Y(\omega)} \right) \right] \right)^{-1}, \tag{13}$$

where the prime denotes the derivative with respect to ω. This equation is actually general, provided that the appropriate complex velocity V and complex modulus Y are used. From the Figures, it can be seen that group and phase velocity coincide at the low and high frequency limits (elastic behaviour).

A constant state of stress instantaneously produced in a previously relaxed specimen with the resulting increasing strain being monitored as a function of the time and following the crea-

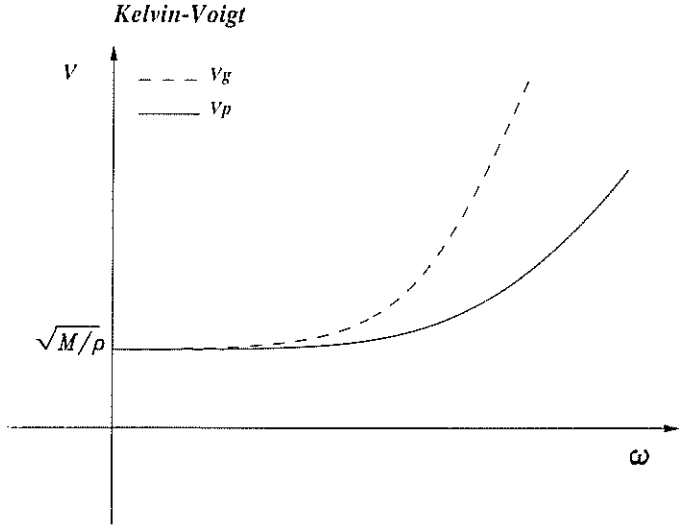

Fig. 10 — Phase and group velocities of the Kelvin-Voigt model. The elastic velocity is obtained at the low frequency limit. High frequencies propagate with infinite velocity.

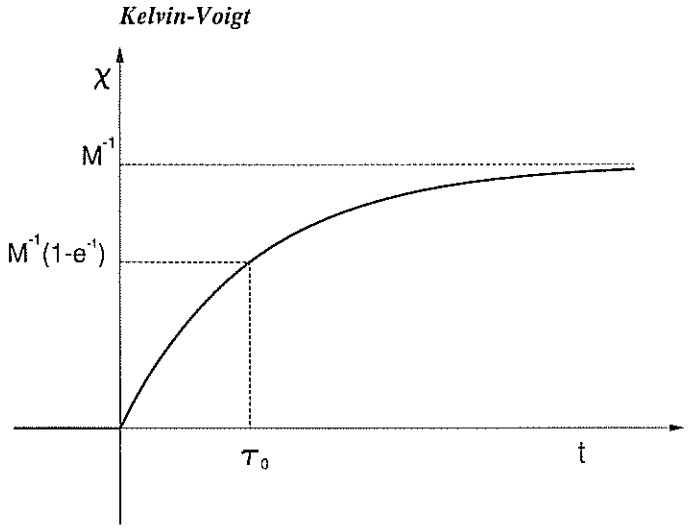

Fig. 11 — The creep function of the Kelvin-Voigt solid lacks the instantaneous response of real solids.

tion of the stressed state describes the creep experiment. The resulting time function is called the creep function. Let us perform the creep experiment on the Maxwell solid. Suppose a unit stress is suddenly applied at $t=0$; the solution of eqn. (9) corresponding to this condition is the creep function

$$\chi\,(t)=\frac{1}{M}\,(1+\frac{t}{\tau_0})\,H\,(t), \tag{14}$$

where $H\,(t)$ is the step function. Alternatively, the stress relaxation experiment consists of a rapidly imposed fixed strain in a previously relaxed specimen. The resulting stress is followed as a function of time for the duration of the applied strain. The experiment gives the relaxation function. Suppose a unit strain is suddenly applied at $t=0$; the resulting relaxation function solution of eqn. (9) is

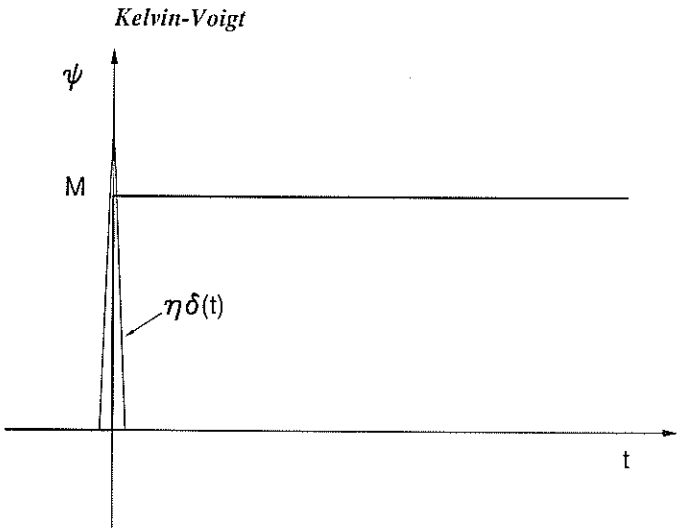

Fig. 12 — The relaxation function of the Kelvin-Voigt model presents an almost elastic behaviour.

$$\psi(t)=Me^{-t/\tau_0}\ H(t). \tag{15}$$

The creep and relaxation functions of the Maxwell solid are depicted in Figs. 6 and 7, respectively. As can be seen, the creep function is not representative of the real creep behaviour in real solids, but resembles the creep function of a viscous fluid. In the relaxation experiment, at $t=0$ both elements experience the same force, and because it is not possible to have an instantaneous deformation in the dashpot, the extention is initially in the spring. Then, the dashpot extends and the spring contracts, such that the total elongation remains constant. At the end of the process, the force in the spring relaxes completely and the relaxation function does not represent an asymptotical residual stress, as in the case of real solids. In conclusion, the Maxwell model appears more appropriate for representing a viscoelastic fluid.

Kelvin-Voigt model

A viscoelastic system commonly used to describe anelastic effects is the Kelvin-Voigt model, which consists of a spring and a dashpot connected in parallel (Fig. 8). The total stress is composed of an elastic stress $\sigma_1=M\epsilon$, and a viscous stress $\sigma_2=\eta\dot{\epsilon}$, where ϵ is the total strain of the system. The constitutive relation becomes

$$\sigma=M\epsilon+\eta\dot{\epsilon}. \tag{16}$$

The Fourier transform of (16) yields

$$\tilde{\sigma}=M(1+i\omega\tau_0)\tilde{\epsilon}. \tag{17}$$

The complex modulus of the Kelvin-Voigt model is then

$$Y(\omega)=M(1+i\omega\tau_0), \tag{18}$$

and the spatial quality factor is

$$Q(\omega)=(\omega\tau_0)^{-1}. \tag{19}$$

Comparing eqn. (12) with (19) shows that the quality factors of the Kelvin-Voigt and Maxwell models are reciprocal functions. The dissipation factor of the Kelvin-Voigt solid is displayed in Fig. 9. The Kelvin-Voigt solid can be used to approximate the left slope of a real relaxation peak.

As with the Maxwell model, the phase velocity is computed by introducting the complex modulus (18) into eqn. (8). It can be seen that the phase velocity $V_p\rightarrow(M/\varrho)^{1/2}$ for $\omega\rightarrow 0$, and $V_p\rightarrow\infty$ when $\omega\rightarrow\infty$, which implies that a wave in a Kelvin-Voigt model travels faster than a wave in an elastic material (see Fig. 10). The group velocity can be computed from eqn. (13). Both phase and group velocities are represented in Fig. 10.

The creep and relaxation experiments on the Kelvin-Voigt solid yield the following creep and relaxation functions:

$$\chi(t)=\frac{1}{M}(1-e^{-t/\tau_0}), \tag{20}$$

and

$$\psi(t)=MH(t)+\eta\delta(t), \tag{21}$$

where $\delta(t)$ is the delta function. The two functions are represented in Figs. 11 and 12, respectively. The relaxation function does not show any time dependence. This is the case of purely elastic solids. The delta function implies that in practice it is impossible to impose an instantaneous strain on the Kelvin-Voigt solid. In the creep experiment, initially the dashpot extends

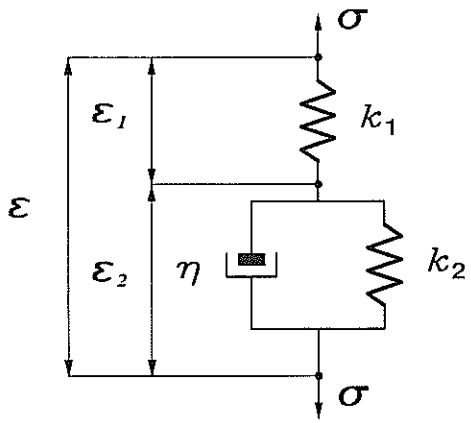

Fig. 13 — Standard linear solid mechanical model.

and begins to transfer the stress to the spring, and at the end, the entire stress is on the spring. The creep function does not present an instantaneous strain at $t=0$ because the dashpot cannot move instantaneously. This is not the case of real solids.

Standard linear solid model

A series combination of a spring and a Kelvin-Voigt model gives a more realistic representation of viscoelastic materials. The resulting system is called standard linear solid and is represented in Fig. 13. The quantities k_1 and k_2 are the elastic constants of the springs. After some calculation, the constitutive relation can be expressed as

$$\sigma+\tau_\sigma\dot{\sigma}=M_R(\epsilon+\tau_\epsilon\dot{\epsilon}), \tag{22}$$

where

$$M_R=\frac{k_1k_2}{k_1+k_2} \tag{23}$$

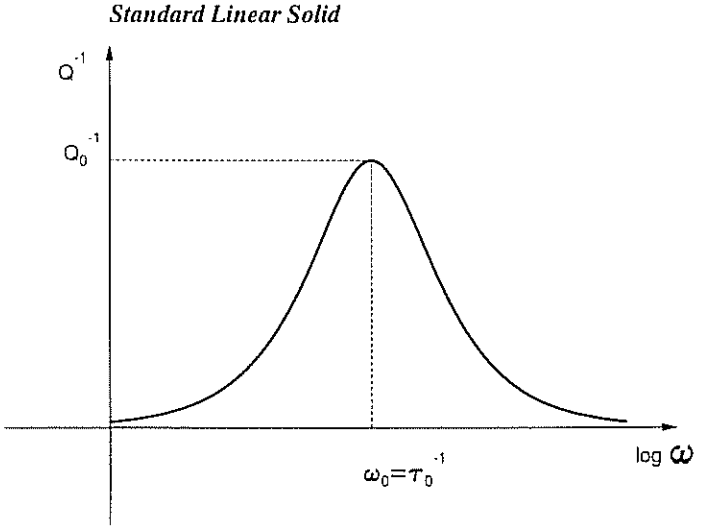

Fig. 14 — The dissipation factor of the standard linear solid represents typical relaxation peaks in solids.

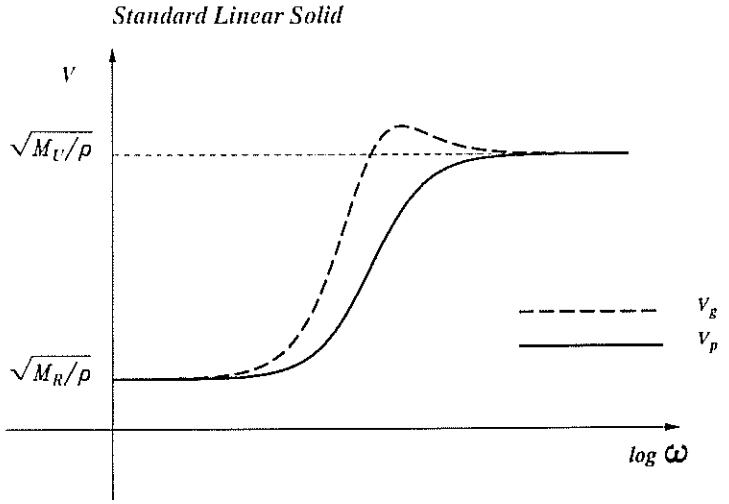

Fig. 15 — Phase and group velocities of the standard linear solid. The limits are the relaxed velocity at low frequencies and the unrelaxed velocity at high frequencies.

is the relaxed modulus, and τ_σ and τ_ϵ are the relaxation times given by

$$\tau_\sigma = \frac{\eta}{k_1 + k_2}, \quad \tau_\epsilon = \frac{\eta}{k_2}. \tag{24}$$

As in the previous models, the complex modulus is obtained from eqn. (22) by performing a Fourier transform. It yields

$$Y(\omega) = M_R \frac{1 + i\omega\tau_\epsilon}{1 + i\omega\tau_\sigma}. \tag{25}$$

The spatial quality factor is given by

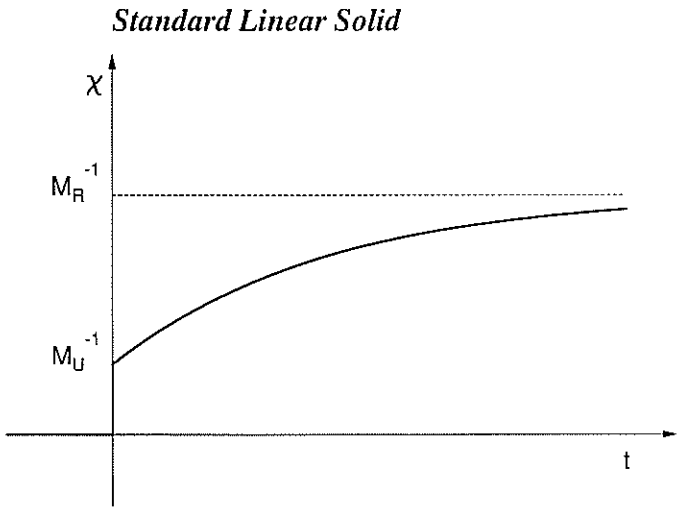

Fig. 16 The creep function of the standard linear solid model presents an instantaneous response and a finite asymptotic value as in real solids.

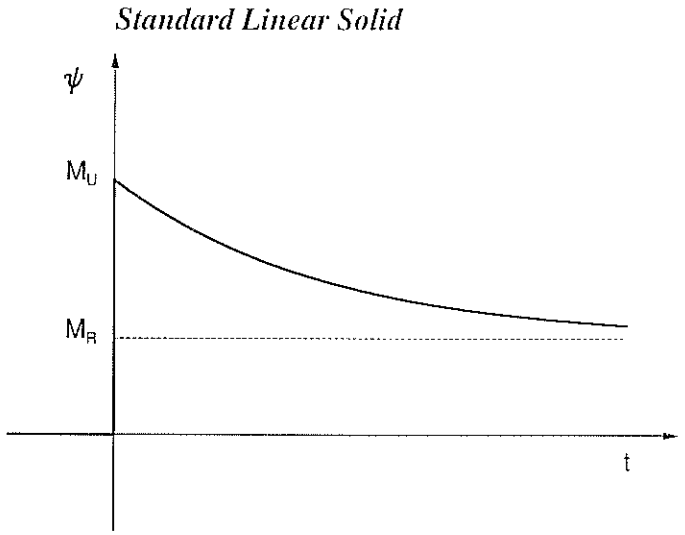

Fig. 17 The relaxation function of the standard linear solid presents an instantaneous unrelaxed state, and at the end of the process the system has relaxed completely to the relaxed modulus M_R.

$$Q(\omega) = \frac{1+\omega^2 \tau_\epsilon \tau_\sigma}{\omega(\tau_\epsilon - \tau_\sigma)} . \tag{26}$$

The dissipation factor of the standard linear solid is displayed in Fig. 14. The standard linear solid presents a single relaxation peak at $\omega_0 = 1/\tau_\sigma$, and therefore, is a suitable model to represent relaxation mechanisms such as those of Fig. 1. Processes such as grain boundary relaxation have to be explained by a distribution of relaxation peaks. This behaviour is obtained by considering several standard linear elements in series or in parallel, a system which is described in the next section. The phase velocity is plotted in Fig. 15 together with the group velocity. The phase velocity variation with frequency ranges from the elastic velocity $(M_R/\varrho)^{1/2}$, also called the relaxed velocity, as $\omega \to 0$, to the unrelaxed velocity $(M_U/\varrho)^{1/2}$ at $\omega = \infty$, where

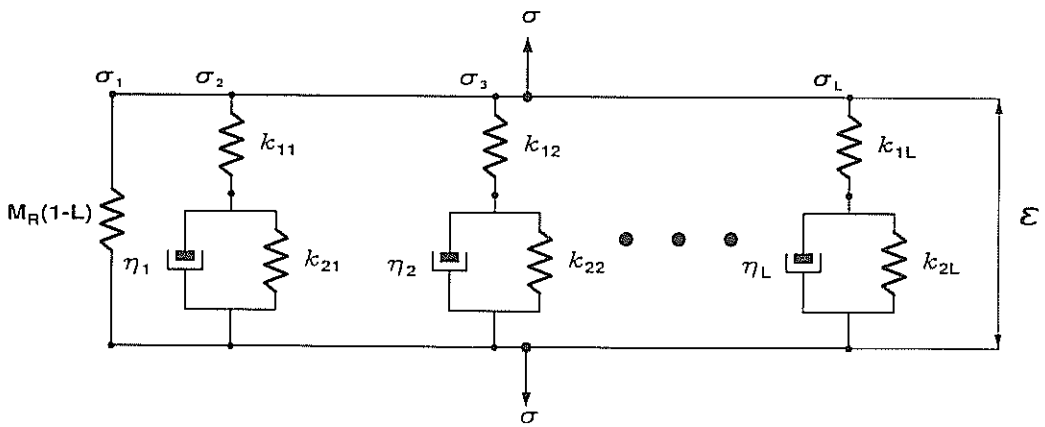

General Standard Linear Solid (Liu et al.)

Fig. 18 — Liu et al.'s mechanical model has a spring with negative constant of value M_R $(1-L)$, where L is the number of standard linear solid elements.

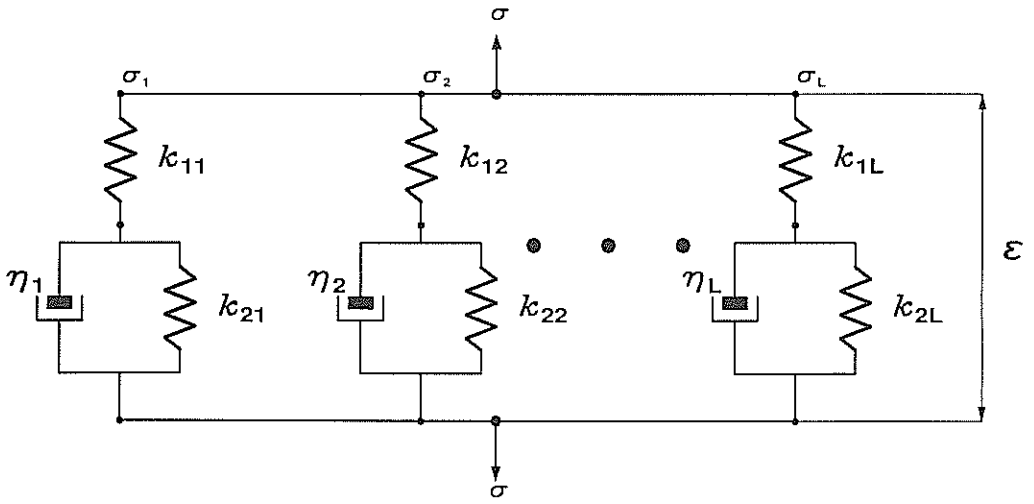

General Standard Linear Solid (1)

Fig. 19 — General standard linear solid model composed of L single elements connected in parallel. The same strain acts on each element.

$$M_U = M_R \frac{\tau_\epsilon}{\tau_\sigma} \tag{27}$$

is the unrelaxed modulus. The meaning of relaxed and unrelaxed moduli becomes clear in the explanation of the creep and relaxation functions. If a constant unit stress is suddenly applied at $t=0$, the solution of eqn. (22) gives the following creep function:

$$\chi(t) = \frac{1}{M_R}\left[1-\left(1-\frac{\tau_\sigma}{\tau_\epsilon}\right)e^{-t/\tau_\epsilon}\right]H(t). \tag{28}$$

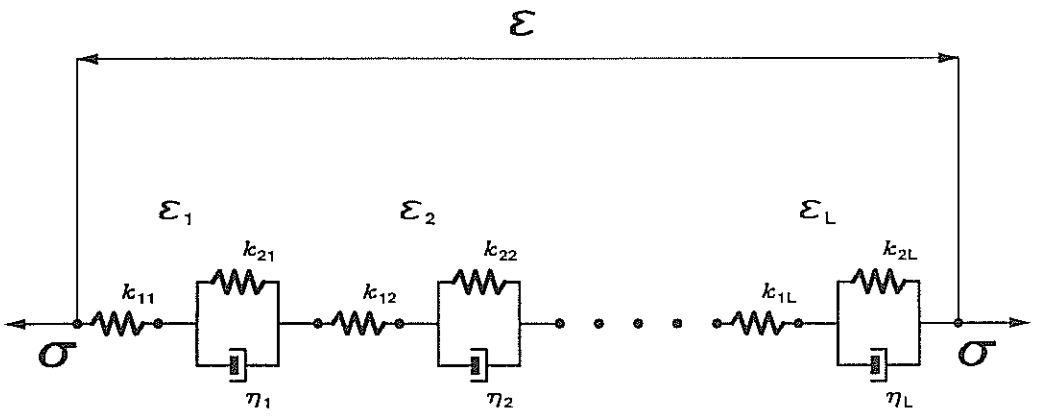

General Standard Linear Solid Model (2)

Fig. 20 — General standard linear solid model composed of L single elements connected in series. The same stress acts on each element.

The solution for unit stress is obtained using the symmetry of the stress-strain relation (22). Exchanging the roles of τ_σ and τ_ϵ, and substituing M_R^{-1} for M_R in eqn. (28), the relaxation function is

$$\psi(t)=M_R\left[1-\left(1-\frac{\tau_\epsilon}{\tau_\sigma}\right)e^{-t/\tau_\sigma}\right]H(t). \tag{29}$$

The creep and relaxation functions are represented in Figs. 16 and 17, respectively. In the creep experiment, there is an istantaneous initial value $\chi(0^+)=M_U^{-1}=k_1^{-1}$, and an asymptotic strain $\chi(\infty)=M_R^{-1}$ determined solely by the spring constants. After the first initial displacement, the force across the dashpot is gradually relaxed by deformation therein, resulting in a gradual increase in the observed overall deformation; finally, the asymptotic value is reached. Similarly, the relaxation function presents an instantaneous unrelaxed state of magnitude M_U, and at the end of the process the system has relaxed completely to the relaxed modulus M_R. Such a system, therefore, manifests the general features of the experimental creep function illustrated in Fig. 2.

Generalized standard linear solid model

As stated before, some processes, as for example grain boundary relaxation, have a dissipation factor which is much broader than a single relaxation curve. It seems natural to try to explain this broadening with a distribution of relaxation mechanisms. This approach was introduced by Liu et al. (1976) in an attempt to obtain a nearly constant quality factor over the seismic frequency range. Their model is represented in Fig. 18, where the first spring in parallel has negative constant. We consider the parallel and series systems represented in Figs. 19 and 20, respectively, with L the number of single standard linear elements. For the first system, the stress-strain relation for each single mechanism is

$$\sigma_l+\tau_{\sigma l}\dot{\sigma}_l=M_{Rl}(\epsilon+\tau_{\epsilon l}\dot{\epsilon}), \tag{30}$$

Where the relaxed moduli M_{Rl} are given by

$$M_{Rl}=\frac{k_{1l}k_{2l}}{k_{1l}+k_{2l}}, \quad l=1,\ldots,L \tag{31}$$

and the relaxation times by

$$\tau_{\sigma l}=\frac{\eta_l}{k_{1l}+k_{2l}}, \quad \tau_{\epsilon l}=\frac{\eta_l}{k_{2l}}, \quad l=1,\ldots,L. \tag{32}$$

The total stress acting on the system is $\sigma=\sum_{l=1}^{L}\sigma_l$; therefore the stress-strain relation in the frequency domain is

$$\tilde{\sigma}(\omega)=\sum_{l=1}^{L}Y_l(\omega)\,\tilde{\epsilon}(\omega)=\sum_{l=1}^{L}M_{Rl}\frac{1+i\omega\tau_{\epsilon l}}{1+i\omega\tau_{\sigma l}}\tilde{\epsilon}(\omega), \tag{33}$$

where expression (25) for a single complex modulus Y_l has been used. Defining $M_{Rl}=M_R/L$, $l=1,\ldots,L$, the complex modulus of the system is

$$Y(\omega)=\frac{M_R}{L}\sum_{l=1}^{L}\frac{1+i\omega\tau_{\epsilon l}}{1+i\omega\tau_{\sigma l}} \tag{34}$$

As before, quality factor and velocities are computed by using eqns. (7), (8) and (13). The relaxation function is easily obtained from the time-domain constitutive equation

$$\sigma(t) = \sum_{l=1}^{L} \sigma_l(t) = \sum_{l=1}^{L} \psi_l(t) * \dot{\epsilon}(t). \tag{35}$$

Hence,

$$\psi(t) = \sum_{l=1}^{L} \psi_l(t) = M_R \left[1 - \frac{1}{L} \sum_{l=1}^{L} \left(1 - \frac{\tau_{\epsilon l}}{\tau_{\sigma l}} \right) e^{-t/\tau_{\sigma l}} \right] H(t). \tag{36}$$

On the other hand, for the series connection (i.e., Fig. 20), the calculation of the creep compliance modulus is straightforward since

$$\tilde{\epsilon}(\omega) = \sum_{l=1}^{L} J_l(\omega)\, \tilde{\sigma}(\omega) = \sum_{l=1}^{L} \frac{1}{M_{Rl}} \frac{1+i\omega\tau_{\sigma l}}{1+i\omega\tau_{\epsilon l}} \tilde{\sigma}(\omega), \tag{37}$$

where the property $J_l = Y_l^{-1}$ has been used. If we assume that $M_{Rl} = M_R L$, the creep modulus is

$$J(\omega) = \frac{1}{M_R L} \sum_{l=1}^{L} \frac{1+i\omega\tau_{\sigma l}}{1+i\omega\tau_{\epsilon l}}, \tag{38}$$

whose creep function is

$$\chi(t) = \frac{1}{M_R} \left[1 - \frac{1}{L} \sum_{l=1}^{L} \left(1 - \frac{\tau_{\sigma l}}{\tau_{\epsilon l}} \right) e^{-t/\tau_{\epsilon l}} \right] H(t). \tag{39}$$

Applying the same calculation to Liu et al.'s model yields the following complex relaxation modulus and relaxation function:

$$Y(\omega) = M_R \left[1 - L + \sum_{l=1}^{L} \frac{1+i\omega\tau_{\epsilon l}}{1+i\omega\tau_{\sigma l}} \right] \tag{40}$$

and

$$\psi(t) = M_R \left[1 - \sum_{l=1}^{L} \left(1 - \frac{\tau_{\epsilon l}}{\tau_{\sigma l}} \right) e^{-t/\tau_{\sigma l}} \right] H(t). \tag{41}$$

The complex moduli (34), (38) and (40) have branch points in the upper half of the ω-plane (considering ω as a complex variable) at

$$\omega_{1l} = \frac{i}{\tau_{\sigma l}}, \quad \omega_{2l} = \frac{i}{\tau_{\epsilon l}}, \quad l = 1, \ldots, L. \tag{42}$$

Consequently $Y(\omega)$ is an analytic function in the lower ω-plane. Thus, the system's impulse

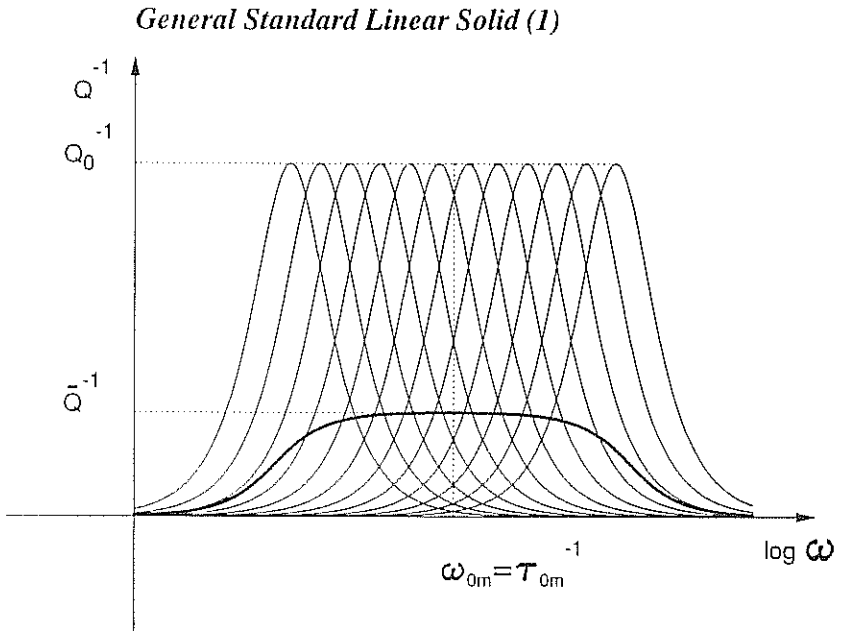

Fig. 21 — A constant-Q model can be constructed with a parallel connection of standard linear solid elements. In this case $Q \gg 1$, the system is composed of L relaxation peaks of maximum value Q_0^{-1} each, and equally distributed in the log (ω) scale. The algorithm is outlined in Appendix B.

response is real and causal, and therefore the Kramers-Kroning dispersion relations are valid. This is also a consequence of the causality principle which is inherent in Boltzmann's superposition principle (Ben-Menahem and Singh, 1981). Fig. 21 displays the dissipation factor of the system represented in Fig. 19. The procedure to obtain an almost constant value $\bar{Q}^{-1}$ in the frequency band of interest is outlined in Appendix B. In particular, this curve is composed of 12 single mechanisms each with maximum dissipation factor Q_0^{-1}. The velocities are represented in Fig. 22. They range from the low frequency value $(M_R / \varrho)^{1/2}$ to the high frequency value $(M_U / \varrho)^{1/2}$, where the unrelaxed mudulus is

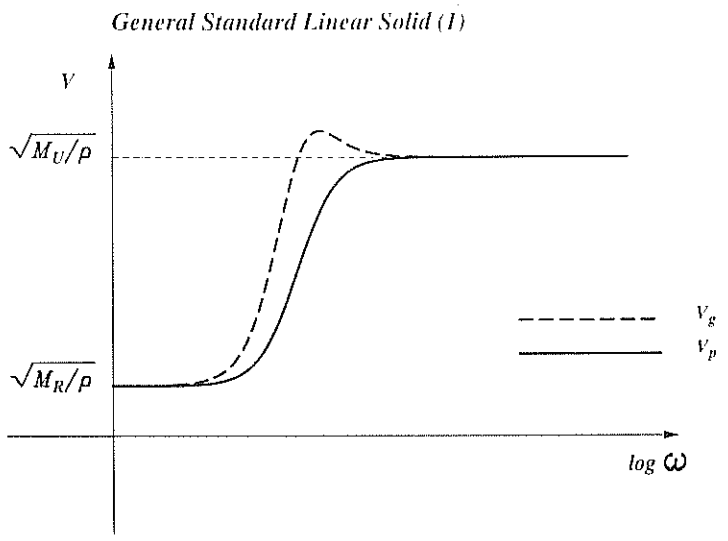

Fig. 22 — Phase and group velocities of the general standard linear solid for the constant-Q model.

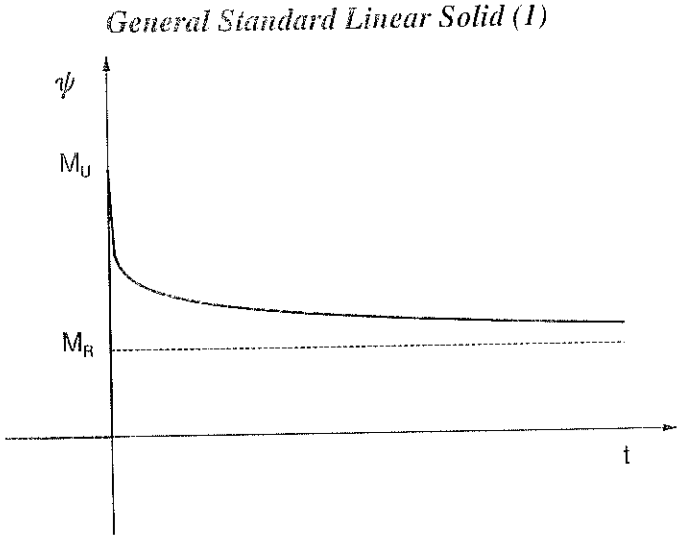

Fig. 23 — Relaxation function of the general standard linear solid composed of L elements connected in parallel (constant-Q model).

$$M_U = M_R \left[1 - \frac{1}{L} \sum_{l=1}^{L} \left(1 - \frac{\tau_{el}}{\tau_{\sigma l}} \right) \right]. \tag{43}$$

The relaxation function of system 1, for an almost constant quality factor, is shown in Fig. 23. Fig. 24 represents the creep function for system 2, where

$$M_U = M_R \left[1 - \frac{1}{L} \sum_{l=1}^{L} \left(1 - \frac{\tau_{\sigma l}}{\tau_{el}} \right) \right]^{-1} \tag{44}$$

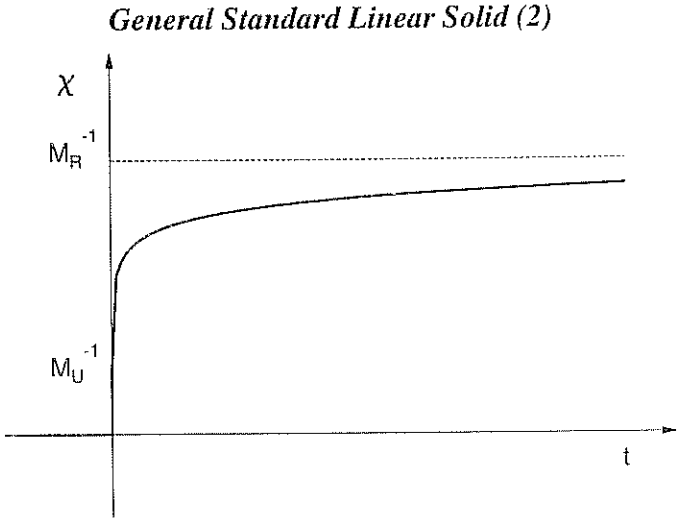

Fig. 24 Creep function of the general standard linear solid composed of L elements connected in series (constant-Q model). The curve is very similar to the experimental creep function shown in Fig. 2.

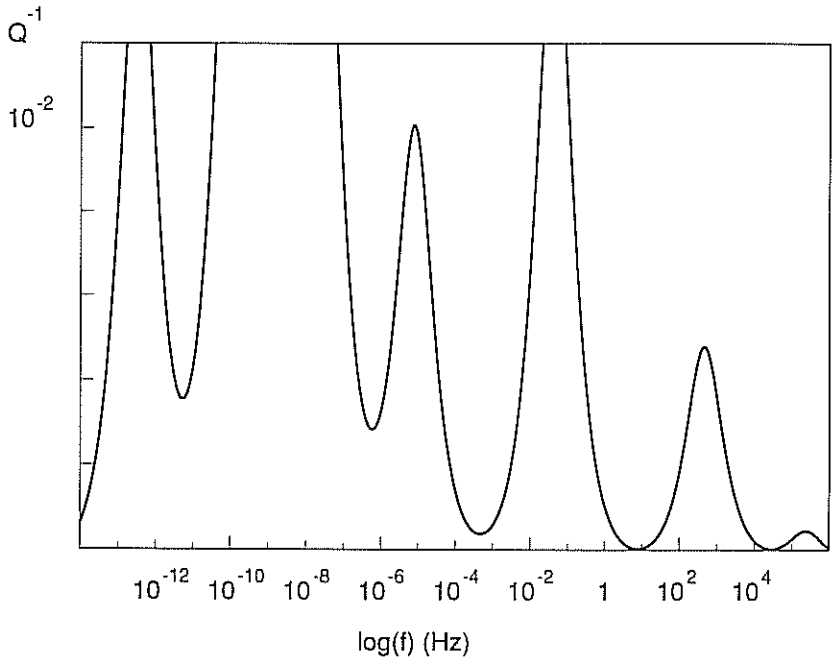

Fig. 25 — The experimental relaxation spectrum of Fig. 1 is reproduced here by using the relaxation times of Table 1. The mechanical model is that represented in Fig. 19. Grain boundary relaxation, for instance, requires several mechanisms.

Table — Relaxation times defining the relaxation spectrum of Fig. 25.

	Relaxation times (seconds)	
	τ_{el}	τ_{al}
Pairs of Solute Atoms	$3.199\times10^{+11}$	$3.167\times10^{+11}$
Grain Boundary	$1.624\times10^{+9}$	$1.560\times10^{+9}$
	$8.138\times10^{+8}$	$7.819\times10^{+8}$
	$4.079\times10^{+8}$	$3.919\times10^{+8}$
	$2.044\times10^{+8}$	$1.964\times10^{+8}$
	$1.025\times10^{+8}$	$9.843\times10^{+7}$
	$5.135\times10^{+7}$	$4.933\times10^{+7}$
	$2.573\times10^{+7}$	$2.473\times10^{+7}$
	$1.290\times10^{+7}$	$1.239\times10^{+7}$
	$6.464\times10^{+6}$	$6.211\times10^{+6}$
	$3.240\times10^{+6}$	$3.113\times10^{+6}$
Twin Boundaries	$1.597\times10^{+4}$	$1.586\times10^{+4}$
Interstitial Solute Atoms	3.199	3.167
Transverse Thermal Currents	3.188×10^{-4}	3.178×10^{-4}
Intercrystalline Thermal Currents	6.368×10^{-7}	6.365×10^{-7}

A set of elements gives a more realistic behaviour of the creep function, as can be seen by comparison with the experimental curve shown in Fig. 2. The experimental relaxation spectrum of Fig. 1 is modelled by the relaxation times listed in the Table. The relaxation times of single peaks can be computed from eqns. B.5 and B.6, from the frequency location at the peak ω_0 and the maximum value Q_0^{-1}. Broad peaks involve several mechanisms and can be computed in the same way as the constant Q-model. The relaxation spectrum, defined by the relaxation times of the Table, is represented in Fig. 25.

CONCLUSIONS

Most of the properties analysed here can be found scattered through many books and articles. In this work, however, we have collected the main features of viscoelastic models related to wave propagation; properties which are associated with the quality factor and phase and group velocities. The anelastic characteristics of a real medium can be described appropriately by a parallel or series connection of standard linear elements. From the location and maximum value of the experimental relaxation peaks as a function of frequency, it is a simple task to compute the associated relaxation times, and build in this way the relaxation spectrum. Similarly, the constant Q model ($Q \gg 1$) can be easily computed with a simple formula without requiring the use of curve fitting techniques. The article also attempts to be a didactic guide for those who wish to introduce anelastic effects into the wave equation.

Acknowledgments. This work was supported in part by the Commission of the European Communities under the GEOSCIENCE project.

REFERENCES

Ben-Menahem A. and Singh S.G.; 1981: *Seismic waves and sources*. Springer Verlag, New York.

Bracewell R.; 1965: *The Fourier transform and its applications*. McGraw-Hill, New York.

Carcione J.M., Kosloff D. and Kosloff R.; 1988a: *Wave propagation simulation in a linear viscoacoustic medium*. Geophys. J.R. astr. Soc., **93**, 393-407.

Carcione J.M., Kosloff D. and Kosloff R.; 1988b: *Wave propagation simulation in a linear viscoelastic medium*. Geophys. J.R. astr. Soc., **95**, 597-611.

Christensen R.M.; 1982: *Theory of viscoelasticity*. An Introduction Academic Press, New York.

Flugge W.; 1960: *Viscoelasticity*. Blaisdell, New York.

Liu H., Anderson D.L. and Kanamori H.; 1976: *Velocity dispersion due to anelasticity; implications for seismology and mantle composition*. Geophys. J.R. astr. Soc., **47**, 41-58.

Maxwell J.C.; 1868: *On the dynamical theory of gases*. Phil. Mag., **35**, 129-145.

Meyer O.E.; 1878: *Über die elastische Nachwirkung*. Ann. Physik u. Chemie, **4** 249-267.

Thomson W. (Lord Kelvin); 1875: Math. Phys. Papers, **3**, 27.

Voigt W.; 1892: *Über innere Reibung fester Körper, insbesondere der Metalle*. Ann. d. Phys., XLVII, 671.

Zener C.; 1948: *Elasticity and anelasticity of metals*. University of Chicago Press, Chicago, Illinois.

APPENDIX A

Complex, phase and group velocities

From the correspondence principle (Flugge, 1960), and from the stress-strain relation (3), one can identify a complex velocty as

$$V(\omega) = \sqrt{\frac{Y(\omega)}{\varrho}} \quad . \tag{A.1}$$

Hence, the complex wavenumber is

$$k = \frac{\omega}{V} \quad . \tag{A.2}$$

The real wavenumber $\varkappa = \mathrm{Re}\,(k)$ can be expressed in terms of the complex velocity as

$$\varkappa = \omega\ \mathrm{Re}\,[V^{-1}] \, . \tag{A.3}$$

The phase velocity is the frequency divided by the real wavenumber:

$$V_p = \frac{\omega}{\varkappa} = \left(\mathrm{Re} \left[V^{-1} \right] \right)^{-1}, \tag{A.4}$$

and the group velocity, i.e. the velocity of the wave packet is given by

$$V_g = \frac{d\omega}{d\varkappa} = \left(\frac{d\varkappa}{d\omega} \right)^{-1} = \left(\mathrm{Re} \left[V(\omega)^{-1} \left(1 - \frac{\omega}{2} \frac{Y'(\omega)}{Y(\omega)} \right) \right] \right)^{-1}, \tag{A.5}$$

where the prime denotes derivative with respet to ω.

APPENDIX B

Constant Q model for low-loss solids

The standard linear solid quality factor for a single mechanism eqn. (26) can be rewritten as

$$Q=Q_0 \frac{1+\omega^2 \tau_0^2}{2\omega\tau_0} \quad . \tag{B.1}$$

where

$$Q_0=\frac{2\tau_0}{\tau_\epsilon - \tau_\sigma} \tag{B.2}$$

is the minimum value occurring at $\tau_0 = (\tau_\epsilon \tau_\sigma)^{1/2}$. Let us assume that Q_0 and τ_0 are known, as is the case of the experimental curve in Fig. 1. Then, it is a simple task to get the relaxation times from the following two equations:

$$Q_0=\frac{2\tau_0}{\tau_\epsilon - \tau_\sigma} \tag{B.3}$$

$$\tau_0^2=\tau_\epsilon \tau_\sigma \, . \tag{B.4}$$

This gives a second-order equation for the relaxation times whose solutions are

$$\tau_\epsilon = \frac{\tau_0}{Q_0} \left[\sqrt{Q_0^2+1}+1 \right] , \tag{B.5}$$

$$\tau_\sigma = \frac{\tau_0}{Q_0} \left[\sqrt{Q_0^2+1}-1 \right] . \tag{B.6}$$

Now, the problem is to find a set of relaxation times $\tau_{\epsilon l}$ and $\tau_{\sigma l}$, $l=1, \ldots, L$ which gives an almost constant quality factor Q in a given frequency band centered at $\omega_{0m}=\tau_{0m}$, the location of the middle mechanism, which is $m=L/2+1$, L odd. Single relaxation peaks should be taken equidistant in a log (ω) scale. The quality factor for the system shown in Fig. 19 is

$$Q=\frac{\mathrm{Re}\,[Y(\omega)]}{\mathrm{Im}\,[Y(\omega)]} = \mathrm{Re}\left[\sum_{l=1}^{L} Y_l(\omega) \right] \left(\mathrm{Im}\left[\sum_{l=1}^{L} Y_l(\omega) \right] \right)^{-1} , \tag{B.7}$$

where Y_l is the complex modulus for each single element. Since $Q_l=Re\,[Y_l]/Im\,[Y_l]$ is the quality factor for each mechanism, eqn. (B.7) becomes

$$Q=\frac{\sum_{l=1}^{L} Q_l \,\mathrm{Im}\,[Y_l(\omega)]}{\sum_{l=1}^{L} \mathrm{Im}\,[Y_l(\omega)]} \quad . \tag{B.8}$$

Substituting the value of Q_l given by (B.1) into (B.8) yields

$$Q=Q_0 \sum_{l=1}^{L} \left(\frac{1+\omega^2 \tau_{0l}^2}{2\omega\tau_{0_l}} \right) \mathrm{Im}\,[Y_l(\omega)] \left(\sum_{l=1}^{L} \mathrm{Im}\,[Y_l(\omega)] \right)^{-1}, \tag{B.9}$$

where $Q_{0l} \equiv Q_0$ has been assumed. We choose the values of τ_{0l}, $l=1, \ldots, Q$ such that they are regularly distributed in the frequency band of interest. If we find Q_Q which gives a value of Q at ω_{0m}, the resulting general curve will have an almost constant quality factor Q. The relaxation times of this curve are computed from Q_0 and τ_{0l} by using eqns. (B.5) and (B.6). We note that for a single mechanism,

$$\mathrm{Im}\,[Y_l(\omega)] = \frac{\omega(\tau_{\epsilon l}-\tau_{\sigma l})}{1+\omega^2 \tau_{\sigma l}^2} = \frac{2\omega\tau_{0l}}{Q_0(1+\omega^2 \tau_{\sigma l}^2)} \tag{B.10}$$

by virtue of eqn. (B.3). For low-loss solids, $\tau_{\sigma l} \cong \tau_{0l}$, and (B.10) becomes

$$\mathrm{Im}\,[Y_l(\omega)] = \frac{2\omega\tau_{0l}}{Q_0(1+\omega^2 \tau_{0l}^2)} \quad . \tag{B.11}$$

Substituting (B.11) into eqn. (B.9) gives

$$Q=Q_0 L \left(\sum_{l=1}^{L} \frac{2\omega\tau_{0l}}{1+\omega^2 \tau_{0l}^2} \right)^{-1}. \tag{B.12}$$

As pointed out before, we take $Q(\omega_{0m})=\overline{Q}$; thus

$$Q_0 = \frac{\overline{Q}}{L} \sum_{l=1}^{L} \frac{2\omega_{0m}\tau_{0l}}{1+\omega_{0m}^2 \tau_{0l}^2} \tag{B.13}$$

gives an almost constant quality factor $\overline{Q}$.